

Dependence of nonlocal Gilbert damping on the ferromagnetic layer type in ferromagnet/Cu/Pt heterostructures

A. Ghosh,¹ J. F. Sierra,¹ S. Auffret,¹ U. Ebels,¹ and W. E. Bailey^{2,a)}

¹SPINTEC, UMR (8191) CEA/CNRS/UJF/Grenoble INP; INAC, 17 rue des Martyrs, 38054 Grenoble Cedex, France

²Department of Applied Physics and Applied Mathematics, Columbia University, New York, New York 10027, USA

(Received 24 November 2010; accepted 8 January 2011; published online 2 February 2011)

We have measured the size effect in the nonlocal Gilbert relaxation rate in ferromagnet (FM) (t_{FM})/Cu(3 nm)/[Pt(2 nm)]/Al(3 nm) heterostructures, FM={Ni₈₁Fe₁₉, Co₆₀Fe₂₀B₂₀, pure Co}. A common behavior is observed for three FM layers where the additional relaxation obeys both a strict inverse power law dependence $\Delta G = Kt^n$, $n = -1.04 \pm 0.06$ and a similar magnitude $K = 224 \pm 40$ MHz·nm. As the tested FM layers span an order of magnitude in spin diffusion length λ_{SD} , the results are in support of spin diffusion rather than nonlocal resistivity as the origin of the effect. © 2011 American Institute of Physics. [doi:10.1063/1.3551729]

The primary materials parameter that describes the temporal response of magnetization M to applied fields H is the Gilbert damping parameter, α , or relaxation rate $G = |\gamma| M_s \alpha$. An understanding of the Gilbert relaxation, particularly in structures of reduced dimension, is an essential question for optimizing the high speed/GHz response of nanoscale magnetic devices.

Experiments over the last decade have established that the Gilbert relaxation of ferromagnetic ultrathin films exhibits a size effect, some component of which is nonlocal. Both $\alpha(t_{FM}) = \alpha_0 + \alpha'(t_{FM})$ and $G(t_{FM}) = G_0 + G'(t_{FM})$ increase several fold with decreasing ferromagnet (FM) film thickness, t_{FM} , from near-bulk values α_0 , G_0 for $t_{FM} \gtrsim 20$ nm. Moreover, the damping size effect can have a nonlocal contribution responsive to layers or scattering centers removed through a nonmagnetic (NM) layer from the precessing FM. Contributed Gilbert relaxation has been seen from other FM layers¹ as well as from heavy-element scattering layers such as Pt.²

The nonlocal damping size effect is strongly reminiscent of the electrical resistivity in ferromagnetic ultrathin films. Electrical resistivity ρ is size-dependent by a similar factor over a similar range of t_{FM} ; the resistivity $\rho(t_{FM})$ is similarly nonlocal, dependent upon layers not in direct contact.³⁻⁵ It is *prima facie* plausible that the nonlocal damping and nonlocal electrical resistivity share a common origin in momentum scattering (with relaxation time τ_M) by overlayers. If the nonlocal damping arises from nonlocal scattering τ_M^{-1} , however, there should be a marked dependence upon the FM layer type. Damping in materials with a short spin diffusion length λ_{SD} is thought to be proportional to τ_M^{-1} (Ref. 6); the claim for “resistivity-like” damping has been made explicitly for Ni₈₁Fe₁₉ by Ingvarsson *et al.*⁷ For a FM with a long λ_{SD} , on the other hand, relaxation G is either nearly constant with temperature or “conductivity-like,” scaling as τ_M .

Interpretation of the nonlocal damping size effect has centered instead on a spin current model⁸ advanced by Tserkovnyak *et al.*⁹ An explicit prediction of this model is that the magnitude of the nonlocal Gilbert relaxation rate ΔG is only

weakly dependent upon the FM layer type. The effect has been calculated¹⁰ as

$$\Delta G = |\gamma|^2 \hbar / 4 \pi (g_{eff}^{\uparrow\downarrow} / S) t_{FM}^{-1} \quad (1)$$

where the effective spin mixing conductance $g_{eff}^{\uparrow\downarrow} / S$ is given in units of channels per area. *Ab initio* calculations predict a very weak materials dependence for the interfacial parameters $g^{\uparrow\downarrow} / S$, with $\pm 10\%$ difference in systems as different as Fe/Au and Co/Cu and negligible dependence on interfacial mixing.¹¹

Individual measurements exist of the spin mixing conductance, through the damping, in FM systems Ni₈₁Fe₁₉,¹² Co,¹³ and CoFeB.¹⁴ However, these experiments do not share a common methodology, which makes a numerical comparison of the results problematic, especially given that Gilbert damping estimates are to some extent model-dependent.¹⁵ In our experiments, we have taken care to isolate the nonlocal damping contribution due to Pt overlayers only, controlling for growth effects, interfacial intermixing, and inhomogeneous losses. The only variable in our comparison of nonlocal damping $\Delta G(t_{FM})$, to the extent possible, has been the identity of the FM layer.

Gilbert damping α has been measured through ferromagnetic resonance (FMR) from $\omega/2\pi = 2-24$ GHz using a broadband coplanar waveguide with broad center conductor width $w = 400$ μm , using field modulation and lock-in detection of the transmitted signal to enhance sensitivity. Magnetic fields H_B are applied in the film plane. The Gilbert damping has been separated from inhomogeneous broadening in the films measured using the well-known relation $\Delta H_{pp}(\omega) = \Delta H_0 + (2/\sqrt{3})\alpha\omega/|\gamma|$. We have fit spectra to Lorentzian derivatives at each frequency, for each film, to extract the linewidth ΔH_{pp} and resonance field H_{res} ; α has been extracted using linear fits to $\Delta H(\omega)$.

For the films, six series of heterostructures were deposited of the form Si/SiO₂/X/FM(t_{FM})/Cu(3 nm)/[Pt(3 nm)]/Al(3 nm), FM={Ni₈₁Fe₁₉ (“Py”), Co₆₀Fe₂₀B₂₀ (“CoFeB”), pure Co}, and $t_{FM} = 2.5, 3.5, 6.0, 10.0, 17.5, 30.0$ nm, for 36 heterostructures included in the study. Samples were deposited by dc magnetron sputtering on thermally oxidized Si (100) substrates with typical depo-

^{a)}Electronic mail: web54@columbia.edu.

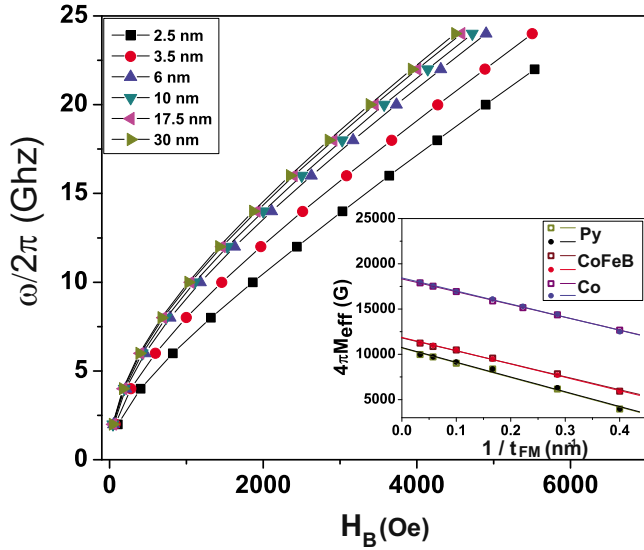


FIG. 1. (Color online) Fields for resonance $\omega(H_B)$ for in-plane FMR, FM = $\text{Ni}_{81}\text{Fe}_{19}$, $2.5 \text{ nm} \leq t_{FM} \leq 30.0 \text{ nm}$; solid lines are Kittel fits. *Inset*: $4\pi M_s^{\text{eff}}$ for all three FM/Cu, with (filled circles) and without (open squares) Pt overlayers.

sition rates of 0.5 \AA/s and Ar pressures of 2.0×10^{-3} mbars. For each ferromagnetic layer type, FM, one thickness series t_{FM} was deposited with the Pt overlayer and one thickness series t_{FM} was deposited without the Pt overlayer. This makes it possible to record the additional damping $\Delta\alpha(t_{FM})$ introduced by the Pt overlayer alone, independent of size effects present in the FM/Cu layers deposited below. In the case of pure Co, a X=Ta(5 nm)/Cu(3 nm) underlayer was necessary to stabilize low-linewidth films; otherwise, depositions were carried out directly upon the *in situ* ion-cleaned substrate.

Field-for-resonance data are presented in Fig. 1. The main panel shows $\omega(H_B)$ data for $\text{Ni}_{81}\text{Fe}_{19}(t_{FM})$. Note that there is a size effect in $\omega(H_B)$: The thinner films have a substantially lower resonance frequency. For $t_{FM}=2.5 \text{ nm}$, the resonance frequency is depressed by $\sim 5 \text{ GHz}$ from $\sim 20 \text{ GHz}$ resonance $H_B \approx 4 \text{ kOe}$. The behavior is fitted to the Kittel relation (lines) $\omega(H_B) = |\gamma| \sqrt{(H_B + H_K)(4\pi M_s^{\text{eff}} + H_B + H_K)}$, where H_K is the effective field from induced anisotropy, found to be $< 10 \text{ Oe}$ in all layers and the inset shows a summary of extracted $4\pi M_s^{\text{eff}}(t_{FM})$ data for the three different FM layers. Samples with (open symbols) and without (closed symbols) Pt overlayers show negligible differences. Linear fits according to $4\pi M_s^{\text{eff}}(t_{FM}) = 4\pi M_s - (2K_s/M_s)t_{FM}^{-1}$ allow the extraction of bulk magnetization $4\pi M_s$ and surface anisotropy K_s ; we find $4\pi M_s^{\text{Py}} = 10.7 \text{ kG}$, $4\pi M_s^{\text{CoFeB}} = 11.8 \text{ kG}$, and $4\pi M_s^{\text{Co}} = 18.3 \text{ kG}$ and $K_s^{\text{Py}} = 0.69 \text{ erg/cm}^2$, $K_s^{\text{CoFeB}} = 0.69 \text{ erg/cm}^2$, and $K_s^{\text{Co}} = 1.04 \text{ erg/cm}^2$. The value of $g_L/2 = |\gamma|/(e/mc)$, $|\gamma| = 2\pi \cdot (2.799 \text{ MHz/Oe}) \cdot (g_L/2)$ is found from the Kittel fits subject to this choice, yielding $g_L^{\text{Py}} = 2.09$, $g_L^{\text{CoFeB}} = 2.07$, and $g_L^{\text{Co}} = 2.15$. The $4\pi M_s$ and g_L values are taken to be size-independent and are in good agreement with bulk values: Extracted $4\pi M_s$ values are slightly larger (by 2%–9%) than those measured by calibrated vibrating sample magnetometry in separate depositions of thick films, and g_L values are typical for the literature.

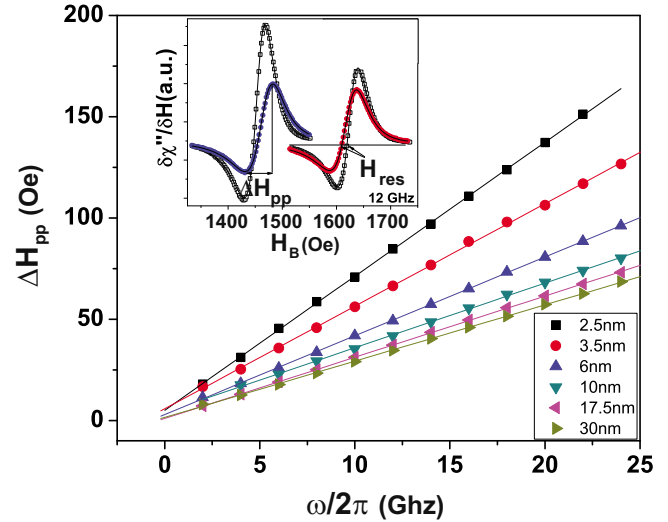


FIG. 2. (Color online) Frequency-dependent peak-to-peak FMR linewidth $\Delta H_{pp}(\omega)$ for FM = $\text{Ni}_{81}\text{Fe}_{19}$, t_{FM} as noted, films with Pt overlayers. *Inset*: Lineshapes and fits for films with (filled circles) and without (open squares) Pt overlayers, FM = $\text{Ni}_{81}\text{Fe}_{19}$ (right), CoFeB (left).

FMR linewidth as a function of frequency $\Delta H_{pp}(\omega)$ is plotted in Fig. 2. The data for Py show a near-proportionality with negligible inhomogeneous component $\Delta H_0 \leq 4 \text{ Oe}$ even for the thinnest layers, facilitating the extraction of intrinsic damping parameter α . The size effect in $\alpha(t_{FM})$ accounts for an increase by a factor of ~ 3 , from $\alpha_0^{\text{Py}} = 0.0067 (G_0^{\text{Py}} = 105 \text{ MHz})$ for the thickest films ($t_{FM} = 30.0 \text{ nm}$) to $\alpha = 0.021$ for the thinnest films ($t_{FM} = 2.5 \text{ nm}$). The inset shows the line shapes for films with and without Pt, illustrating the broadening without significant frequency shift or significant change in peak asymmetry.

A similar analysis has been carried through for CoFeB and Co (not pictured). Larger inhomogeneous linewidths are observed for pure Co, but homogeneous linewidth still exceeds inhomogeneous linewidth by a factor of three over the frequency range studied, and inhomogeneous linewidths agree within experimental error for the thinnest films with and without Pt overlayers. We extract for these films $\alpha_0^{\text{CoFeB}} = 0.0065 (G_0^{\text{CoFeB}} = 111 \text{ MHz})$ and $\alpha_0^{\text{Co}} = 0.0085 (G_0^{\text{Co}} = 234 \text{ MHz})$. The latter value is in very good agreement with the average of easy- and hard-axis values for epitaxial fcc Co films measured up to 90 GHz, $G_0^{\text{Co}} = 225 \text{ MHz}$.¹⁶

We isolate the effect of Pt overlayers on the damping size effect in Fig. 3. Values of α have been fitted for each deposited heterostructure: Each FM type at each t_{FM} for films with and without Pt overlayers. We take the difference $\Delta\alpha(t_{FM})$ for identical FM(t_{FM})/Cu(3 nm)/Al(2 nm) depositions with and without the insertion of Pt(3 nm) after the Cu deposition. Data, as shown on the logarithmic plot in the main panel, are found to obey a power law $\Delta\alpha(t_{FM}) = Kt^n$ with $n = -1.04 \pm 0.06$. This is in excellent agreement with an inverse thickness dependence $\Delta\alpha(t_{FM}) = K_{FM}/t_{FM}$, where the prefactor clearly depends on the FM layer, highest for Py and lowest for Co. Note that efforts to extract $\Delta\alpha(t_{FM}) = Kt^n$ without the FM(t_{FM})/Cu baselines would meet with significant errors; numerical fits to $\alpha(t_{FM}) = Kt_{FM}^n$ for the FM(t_{FM})/Cu/Pt structures yield exponents $n \approx 1.4$.

Expressing now the additional Gilbert relaxation as $\Delta G(t_{FM}) = |\gamma| M_s \Delta\alpha(t_{FM}) = |\gamma^{\text{FM}}| M_s^{\text{FM}} K_{FM}/t_{FM}$, we plot

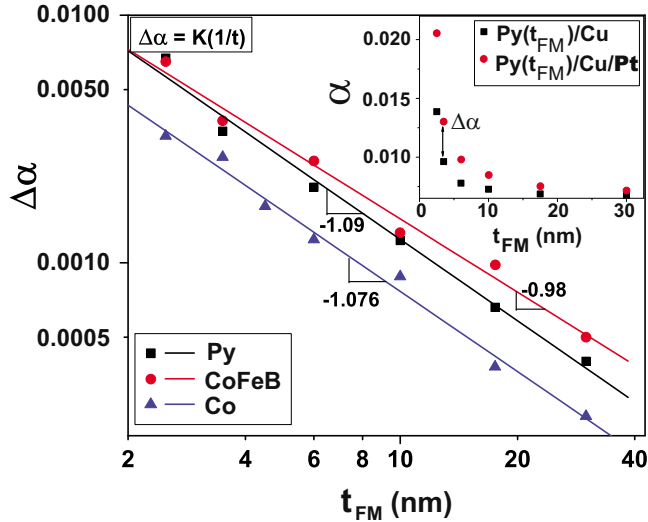


FIG. 3. (Color online) *Inset*: $\alpha_{\text{nopT}}(t_{\text{FM}})$ and α_{Pt} for Py after linear fits to data in Fig. 2. *Main panel*: $\Delta\alpha(t_{\text{FM}}) = \alpha_{\text{Pt}}(t_{\text{FM}}) - \alpha_{\text{nopT}}(t_{\text{FM}})$ for Py, CoFeB, and Co. The slopes express the power law exponent $n = -1.04 \pm 0.06$.

$\Delta G \cdot t_{\text{FM}}$ in Fig. 4. We find $\Delta G \cdot t_{\text{Py}} = 192 \pm 40$ MHz, $\Delta G \cdot t_{\text{CoFeB}} = 265 \pm 40$ MHz, and $\Delta G \cdot t_{\text{Co}} = 216 \pm 40$ MHz. The similarity of values for $\Delta G \cdot t_{\text{FM}}$ is in good agreement with predictions of the spin pumping model in Eq. (1), given that interfacial spin mixing parameters are nearly equal in different systems.

The similarity of the $\Delta G \cdot t_{\text{FM}}$ values for the different FM layers is, however, at odds with expectations from the “resistivity-like” mechanism. In Fig. 4, *inset*, we show the dependence of $\Delta G \cdot t_{\text{FM}}$ upon the tabulated λ_{SD} of these layers from Ref. 17. It can be seen that λ_{SD} is roughly an order of magnitude longer than it is for the other two FM layers, Py and CoFeB, but the contribution of Pt overlayers to damping is very close to their average. Since under the resistivity mechanism, only Py and CoFeB should be susceptible to a resistivity contribution in $\Delta\alpha(t_{\text{FM}})$, the results imply that the contribution of Pt to the nonlocal damping size effect has a separate origin.

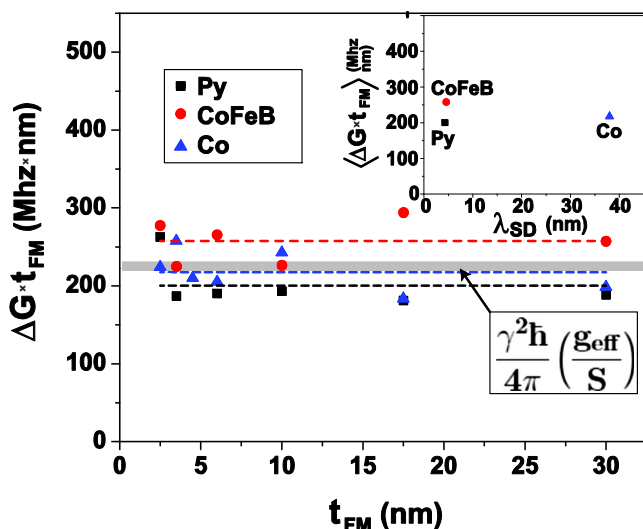


FIG. 4. (Color online) The additional nonlocal relaxation due to Pt overlayers, expressed as a Gilbert relaxation rate—thickness product $\Delta G \cdot t_{\text{FM}}$ for Py, CoFeB, and Co. *Inset*: Dependence of $\Delta G \cdot t_{\text{FM}}$ on spin diffusion length λ_{SD} as tabulated in Ref. 17.

Finally, we compare the magnitude of the nonlocal damping size effect with that predicted by the spin pumping model in Ref. 10. According to $\Delta G \cdot t_{\text{FM}} = |\gamma|^2 \hbar / 4\pi (g_{\text{eff}}^{\uparrow\downarrow} / S) = 25.69 \text{ MHz} \cdot \text{nm}^3 (g_L / 2)^2 (g_{\text{eff}}^{\uparrow\downarrow} / S)$, our experimental $\Delta G \cdot t_{\text{FM}}$ and g_L data yield effective spin mixing conductances $g_{\text{eff}}^{\uparrow\downarrow} / S [\text{Py}/\text{Cu}/\text{Pt}] = 6.8 \text{ nm}^{-2}$, $g_{\text{eff}}^{\uparrow\downarrow} / S [\text{Co}/\text{Cu}/\text{Pt}] = 7.3 \text{ nm}^{-2}$, and $g_{\text{eff}}^{\uparrow\downarrow} / S [\text{CoFeB}/\text{Cu}/\text{Pt}] = 9.6 \text{ nm}^{-2}$. Note that these experimental values are roughly half those reported in Ref. 2 for Py/Cu/Pt. The Sharvin-corrected form in the realistic limit of $\lambda_{\text{SD}}^{\text{N}} \gg t_{\text{N}}$ ¹¹ is $(g_{\text{eff}}^{\uparrow\downarrow} / S)^{-1} = (g_{\text{FN}/\text{N}}^{\uparrow\downarrow} / S)^{-1} - \frac{1}{2} (g_{\text{N},\text{S}}^{\uparrow\downarrow} / S)^{-1} + 2e^2 \hbar^{-1} \rho t_{\text{N}} + (\bar{g}_{\text{N}_1/\text{N}_2}^{\uparrow\downarrow} / S)^{-1}$. Using ideal upper-bound interfacial conductances and bulk resistivities, 14.1 nm^{-2} (Co/Cu), 15.0 nm^{-2} (Cu), 211 nm^{-2} (bulk ρ_{Cu} , $t_{\text{N}} = 3 \text{ nm}$), and 35 nm^{-2} (Cu/Pt) would predict a theoretical $g_{\text{eff},\text{th}}^{\uparrow\downarrow} / S [\text{Co}/\text{Cu}/\text{Pt}] = 14.1 \text{ nm}^{-2}$, as reported in Ref. 2. Our results could be reconciled with the theory through the assumption of more resistive interfaces, plausibly reflective of disorder at the Cu/Pt interface (e.g., $\bar{g}_{\text{Cu}/\text{Pt}}^{\uparrow\downarrow} / S \approx 10 \text{ nm}^{-2}$).

To summarize, a common methodology, controlling for damping size effects and intermixing in single films, has allowed us to compare the nonlocal damping size effect in different FM layers. We observe for Cu/Pt overlayers the same power law in thickness $t^{-1.04 \pm 0.06}$, the same materials independence but roughly half the magnitude that is predicted by the spin pumping theory of Tserkovnyak in the limit of perfect interfaces.¹⁰ The rough independence on FM spin diffusion length, shown here for the first time, argues against a resistivity-based interpretation for the effect.

We thank Y. Tserkovnyak for discussions. We would like to acknowledge the U.S. NSF-ECCS-0925829, the Bourse Accueil Pro no. 2715 of the Rhône-Alpes Region, the French National Research Agency (ANR) Grant No. ANR-09-NANO-037, and the FP7-People-2009-IEF program no. 252067.

¹R. Urban, G. Woltersdorf, and B. Heinrich, *Phys. Rev. Lett.* **87**, 217204 (2001).

²S. Mizukami, Y. Ando, and T. Miyazaki, *Phys. Rev. B* **66**, 104413 (2002).

³B. Dieny, J. Nozieres, V. Speriosu, B. Gurney, and D. Wilhoit, *Appl. Phys. Lett.* **61**, 2111 (1992).

⁴W. H. Butler, X.-G. Zhang, D. M. C. Nicholson, T. C. Schulthess, and J. M. MacLaren, *Phys. Rev. Lett.* **76**, 3216 (1996).

⁵W. E. Bailey, S. X. Wang, and E. Y. Tsymbal, *Phys. Rev. B* **61**, 1330 (2000).

⁶V. Kamberský, *Can. J. Phys.* **48**, 2906 (1970).

⁷S. Ingvarsson, L. Ritchie, X. Y. Liu, G. Xiao, J. Slonczewski, P. L. Trouilloud, and R. H. Koch, *Phys. Rev. B* **66**, 214416 (2002).

⁸R. H. Silsbee, A. Janossy, and P. Monod, *Phys. Rev. B* **19**, 4382 (1979).

⁹Y. Tserkovnyak, A. Brataas, and G. E. W. Bauer, *Phys. Rev. Lett.* **88**, 117601 (2002).

¹⁰Y. Tserkovnyak, A. Brataas, G. E. W. Bauer, and B. I. Halperin, *Rev. Mod. Phys.* **77**, 1375 (2005).

¹¹M. Zwierzycki, Y. Tserkovnyak, P. J. Kelly, A. Brataas, and G. E. W. Bauer, *Phys. Rev. B* **71**, 064420 (2005).

¹²S. Mizukami, Y. Ando, and T. Miyazaki, *J. Magn. Magn. Mater.* **239**, 42 (2002); *Jpn. J. Appl. Phys.* **40**, 580 (2001), and references therein.

¹³J.-M. L. Beaujour, W. Chen, A. Kent, and J. Sun, *J. Appl. Phys.* **99**, 08N503 (2006); J.-M. L. Beaujour, J. H. Lee, A. D. Kent, K. Krycka, and C.-C. Kao, *Phys. Rev. B* **74**, 214405 (2006), and references therein.

¹⁴H. Lee, L. Wen, M. Pathak, P. Janssen, P. LeClair, C. Alexander, C. K. A. Mewes, and T. Mewes, *J. Phys. D* **41**, 215001 (2008).

¹⁵R. D. McMichael and P. Krivosik, *IEEE Trans. Magn.* **40**, 2 (2004).

¹⁶F. Schreiber, J. Pflaum, Z. Frait, Th. Müghe, and J. Pelzl, *Solid State Commun.* **93**, 965 (1995).

¹⁷J. Bass and W. P. Pratt, *J. Phys.: Condens. Matter* **19**, 183201 (2007); C. Ahn, K.-H. Shin, and W. Pratt, *Appl. Phys. Lett.* **92**, 102509 (2008), and references therein.